Journal of Materials Science: Materials in Electronics
https://doi.org/10.1007/s10854-020-03294-x

An ultra-low-firing $NaBi_3V_2O_{10}$ ceramic and its dielectric properties at RF and microwave frequency bands

Guangjie Yang[1] · Changzhi Yin[2] · Yanping Kang[2] · Shaohua Zhang[3] · Chunchun Li[2,3]

Received: 25 February 2020 / Accepted: 20 March 2020

Abstract
An ultra-low-firing $NaBi_3V_2O_{10}$ ceramic, fabricated at 620 °C by a solid-state route, was studied in terms of microstructure, dielectric properties, and chemical compatibility with aluminum electrodes for the first time. $NaBi_3V_2O_{10}$ crystalized in a primitive triclinic structure P1 and developed a dense microstructure, and exhibited good chemical compatibility with aluminum. These merits render its potential utilization in low-temperature cofired ceramic technology. However, the microwave dielectric properties of $NaBi_3V_2O_{10}$ are unsatisfactory with $\varepsilon_r \sim 26.0$, $Q \times f \sim 3200$ GHz, and $\tau_f \sim -88.3$ ppm/°C. Based on RF dielectric characterizations of relative permittivity and impedance over a broad frequency and temperature range, the relatively low-quality factor was explained by the oxygen vacancies caused by sintering and Na and Bi volatilization. These results imply an optimization potential in dielectric properties of $NaBi_3V_2O_{10}$ through compositional and processing adjustments. This work also provides an alternative paradigm to evaluate the performances of microwave dielectric properties.

1 Introduction

Microwave dielectric materials have played a key role in the electronics industry with a wide range of applications as dielectric resonators, filters, antennas, dielectric substrates, etc. [1–3]. The recent advances in wireless telecommunication, the Tactile Internet (5G wireless systems), and the Internet of Things (IoT) have resulted in an increasing demand for microwave dielectric materials [4–6]. It is well known that for practical applications, microwave dielectric materials should have an appropriate dielectric constant (high for miniaturization and low for fast signal transmission), high-quality factor ($Q \times f$), and near-zero temperature coefficient of resonant frequency (τ_f) [7–10]. Although numerous excellent microwave dielectric materials have been reported, there remains much interest in searching for novel microwave materials with desirable dielectric performances from both a fundamental and an industrial viewpoint.

On the other hand, over the past two decades, there are considerable interests in low-temperature cofired ceramics (abbreviated as LTCC), owing to its ability for miniaturization and integration [11–14]. In LTCC multilayer devices, alternating dielectric ceramics stack with internal metallic electrode layers. Thus, the microwave dielectric materials are primarily required to have low sintering temperatures to cofire with the commonly used and highly conducting metals (e.g., 960 °C for Ag and 1083 °C for Cu) [15, 16].

Some low-firing oxide compounds with intrinsically low sintering temperature and promising microwave dielectric properties have been developed in the Li_2O-, TeO_2-, Bi_2O_3-, GeO_2-, V_2O_5, WO_3-, and MoO_3-based systems [17–23]. This inspires us to explore promising low-firing microwave dielectric materials in the Na_2O–Bi_2O_3–V_2O_5 system.

$NaBi_3V_2O_{10}$ is one compound in the Na_2O–Bi_2O_3–V_2O_5 system, which was first reported by Sinclair in 1998 [24]. It belongs to a primitive triclinic structure with a space group P1 and undergoes a reversible phase transition at 575 °C. Especially, based on the previous reports [24, 25], $NaBi_3V_2O_{10}$ ceramics are estimated to be densified at extremely low temperatures ~ 600 °C. Although the ion conduction was determined [25, 26], the dielectric properties

✉ Changzhi Yin
ychangzhi@163.com

✉ Chunchun Li
lichunchun2003@126.com

[1] College of Information Science and Engineering, Guilin University of Technology, Guilin 541004, China

[2] College of Material Science and Engineering, Guilin University of Technology, Guilin 541004, China

[3] School of Materials Science and Engineering, Jiangxi Engineering Laboratory for Advanced Functional Thin Films and Jiangxi Key Laboratory for Two-Dimensional Materials, Nanchang University, Nanchang 330031, China

Published online: 06 April 2020

of $NaBi_3V_2O_{10}$ have not been studied. Thus, in this work, $NaBi_3V_2O_{10}$ ceramics were prepared by the solid-state reaction method. The dielectric properties were systematically characterized at radio frequency (RF) and microwave frequencies.

2 Experimental process

Proportionate amounts of reagent-grade raw materials of Na_2CO_3 (> 99.9%, Guo-Yao Co. Ltd., Shanghai, China), Bi_2O_3 (> 99%, Guo-Yao Co. Ltd., Shanghai, China), and V_2O_5 (> 99%, Guo-Yao Co. Ltd., Shanghai, China) were weighted, mixed, and ball-milled in alcohol medium for 4 h in nylon battle with zirconia balls. The powder mixture was dried and calcined at 500 °C for 4 h. Then, the calcined powders were re-milled, added with polyvinyl alcohol (PVA) as the binder, and uniaxially pressed into disks of 12 mm in diameter and 7 mm in thickness under the pressure of 200 MPa. The samples were heated to 550 °C for 4 h to remove the organic binder and then sintered at 600–660 °C for 4 h.

The phase purity and crystal structure were evaluated using an X-ray diffractometry (XRD) (Cu*K*α1, 1.54059 A, Model X'Pert PRO, PANalytical, Almelo, The Netherlands). The microstructure of the samples was observed by a Scanning Electron Microscope (SEM, Model JSM6380–LV, JEOL, Tokyo, Japan). The bulk densities of the ceramics were determined by the Archimedes method. The impedance spectra were recorded in the frequency range of 100 Hz to 1 MHz (Agilent 4294A impedance analyzer) and silver paste was applied on both sides of the ceramics (sintered at 550 °C for 0.5 h). The microwave dielectric properties were measured using a network analyzer (Model N5230A, Agilent Co., Palo Alto, Canada) and a temperature chamber (Delta 9039, Delta Design, San Diego, CA). The temperature coefficients of resonant frequency were calculated by the equation:

$$\tau_f = \frac{f_2 - f_1}{f_1(T_2 - T_1)} \times 10^6 \text{ (ppm/°C)} \quad (1)$$

where f_1 and f_2 represent resonant frequencies at temperatures T_1 and T_2, respectively.

3 Results and discussion

Figure 1 shows the XRD profiles of $NaBi_3V_2O_{10}$ ceramics sintered at various temperatures (600–650 °C) and the cofired ceramic with 20 wt% aluminum (Al) at 620 °C. By indexing with the JCPDS No. 05-1226, all the observed peaks could be identified with no trace of the second phase in the whole sintering temperature range. This result indicates the phase purity and structure stability of $NaBi_3V_2O_{10}$. Considering the extremely low sintering temperature of $NaBi_3V_2O_{10}$, it is considered as a promising candidate in ULTCC application. Thus, the chemical compatibility of $NaBi_3V_2O_{10}$ ceramics with the aluminum electrode is evaluated via cofiring them at 620 °C. XRD profiles, as shown in Fig. 1a, exhibit both the diffraction peaks of the $NaBi_3V_2O_{10}$ and aluminum phase without other phases being detected. SEM picture (Fig. 1b) captured on the cofired sample is characterized by distinct grains with different element contrasts and sizes, from which the large and shaded grains

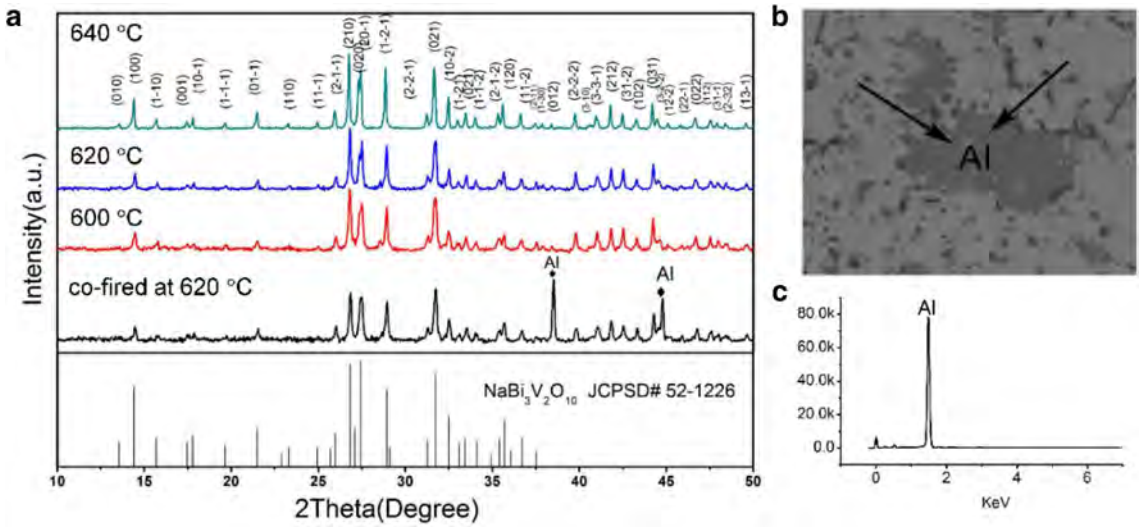

Fig. 1 XRD profiles of **a** $NaBi_3V_2O_{10}$ ceramics sintered at various temperatures (600–650 °C) and **b** the cofired ceramic with 20 wt% aluminum (Al) at 620 °C; **c** EDS for Al electrode in the cofired ceramic

were detected as Al from EDS analysis (Fig. 1c). The combined evidence proves that no chemical reaction took place between them.

Microstructural evolution with sintering temperature is demonstrated in Fig. 2. Over the whole sintering temperature range from 600 to 630 °C, no distinct diversity in SEM images is observed. All samples exhibit a relatively dense microstructure.

As shown in Fig. 3, the sample sintered at 600 °C has a bulk density of 5.85 g/cm^3 being about 92.2% of the theoretical density of 6.35 g/cm^3. As the sintering temperature increased, the bulk density reached the top with a value of 5.96 g/cm^3 (93.9%). Despite the subsequent slight decline in density, all samples exhibit similar values with the relative density being between 92 and 94%, which is consistent with their similar microstructures. The relative permittivity (ε_r) behaved a similar dependence on the sintering temperature and a saturated value of 26.0 was approached. The variation in quality factor ($Q\times f$) with increasing sintering temperature resembled that of bulk density, verifying the dominated influence of bulk density on the dielectric properties. By contrast, no such correlation in the temperature coefficient of resonance frequency (τ_f) on sintering temperature is observed, whereby τ_f exhibited a fluctuant value between − 75 and − 90 ppm/°C. In summary, the best-densified sample at 620 °C possessed the optimized performances with a relative density of 93.9%, and an ε_r of 26.0, a $Q\times f$ of 3200 GHz, and a τ_f of − 88.3 ppm/°C.

Table 1 compares the sintering temperature and microwave dielectric properties of some compounds either Na- or Bi-containing vanadates. By comparison, it is found that Bi-based vanadates have larger relative permittivities with

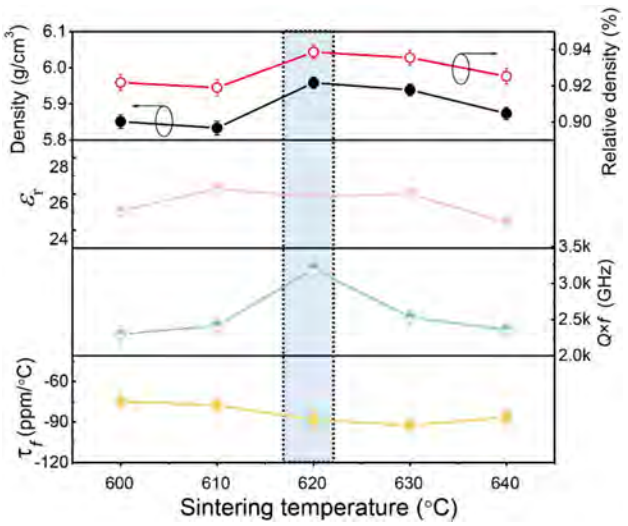

Fig. 3 Variations in density, ε_r, $Q\times f$, and τ_f as a function of sintering temperature from 600 to 640 °C

respect to the Na-containing counterparts, which can be explained by the stereochemical activity of the lone pair electrons of Bi^{3+} that leads to the hybridization between the Bi 6p and O 2p orbits. The same situation is found in $NaBi_3V_2O_{10}$, but the dielectric polarizability is diluted by Na solution, leading to the lower ε_r than that of $BiVO_4$ [39]. Nonetheless, the quality factors of Na-containing vanadates are much higher. Except for $Na_2BiA_2V_3O_{12}$ (A = Zn, Mg), all the listed materials possess a large negative τ_f value, which seems like a common feature for vanadates and needs to be tuned to satisfy the practical applications. It is worth noting that the candidates constituting by both Na_2O and

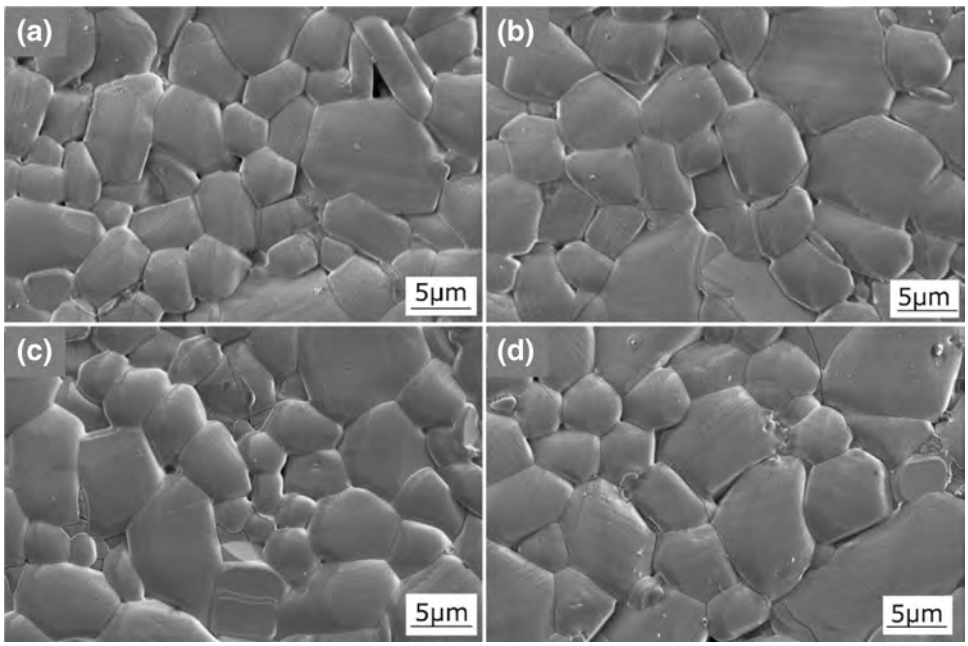

Fig. 2 SEM images of the $NaBi_3V_2O_{10}$ ceramics sintered at various temperatures: **a** 600 °C; **b** 610 °C; **c** 620 °C; **d** 630 °C

Table 1 Sintering temperature and microwave dielectric properties of some compounds either Na- or Bi-containing vanadates

Compound	S.T. (°C)	ε_r	$Q\times f$ (GHz)	τ_f (ppm/°C)	Electrode	References
$BiVO_4$	820	68	8000	−260	React with Ag	[27]
$BiMg_2VO_6$ (A = Cu, Mg)	740–780	13.34–22.7	11,960–15,610	−17.2 to −87.2	Ag	[28]
$BiCaVO_5$ (A = Ca, Mg)	820	15.7–18.6	55,000–86,860	−71 to −65	Ag	[29]
$BiZn_2Li_2V_3O_{12}$	675	17	17,522	−154	No study	[30]
$BiBa_2V_3O_{11}$	880	14.2	68,700	−81	No study	[31]
$NaCa_4V_5O_{17}$	840	9.72	51,000	−84	Ag	[14]
$Na_2AMg_2V_3O_{12}$ (A = Nd, Sm)	850	12–12.1	26,544–36,207	−63 to −69	Ag	[32]
$Na_2Ymg_2V_3O_{12}$	850	12.3	23,180	−4.1	Ag	[33]
$NaMg_4V_3O_{12}$	830	9.53	32,820	−90	No study	[34]
$NaA_2Mg_2V_3O_{12}$ (A = Ca, Sr)	900–915	10–11.7	37,950–50,600	−2.9 to −47	Ag	[35]
$NaPb_2B_2V_3O_{12}$ (A = Zn, Mg)	650–725	20.6–22.4	7900–22,800	−6 to +25.1	No study	[36]
$Na_2BiMg_2V_3O_{12}$	660	23.2	3700	+8.2	No study	[37]
$Na_2BiZn_2V_3O_{12}$	600	22.3	19,960	+15.5	Al, Ag	[38]
$NaBi_3V_2O_{10}$	620	26.0	3200	−88.3	Al	This work

Bi_2O_3, i.e., the present $NaBi_3V_2O_{10}$, have the lowest sintering temperature but inferior $Q\times f$ values compared to those with only Na_2O or Bi_2O_3. Because both Na_2O and Bi_2O_3 have been reported to be volatile under elevated temperatures [14, 40], we speculate the extremely low-quality factor of $NaBi_3V_2O_{10}$ is related to the dielectric losses caused by conductivity from the long-range moving of defects resulting from element volatilization. To verify this propose, RF dielectric characterization in terms of frequency and temperature dependence of relative permittivity and impedance analysis was conducted over a broad range.

Frequency and temperature dependence of dielectric properties verify the existence of defect dipoles in the present system. Orientation polarization of defect dipoles contributes to relative permittivity, especially at low frequencies. It belongs to one of the slow polarizations with a characteristic frequency up to kHz. This feature determines that this kind of polarization only responses at low frequencies, which explains the evident frequency dispersion of relative permittivity and loss tangent of $NaBi_3V_2O_{10}$ sintered at 620 °C, as shown in Fig. 4a. Another feature of the slow polarization is the thermally activated nature, which can be exhibited in the temperature-dependent dielectric properties in Fig. 4b. With increasing measuring temperature, the "freezing" defect dipoles at high frequencies are activated due to the growing thermal motion, and thus, the defect dipoles can follow the frequency switching and give rise to an increase in relative permittivity and losses. Thereafter comes the question that what the defects are and where they are from.

It is well known that oxygen loss in oxides when fired at elevated temperatures is universal, yielding a certain amount

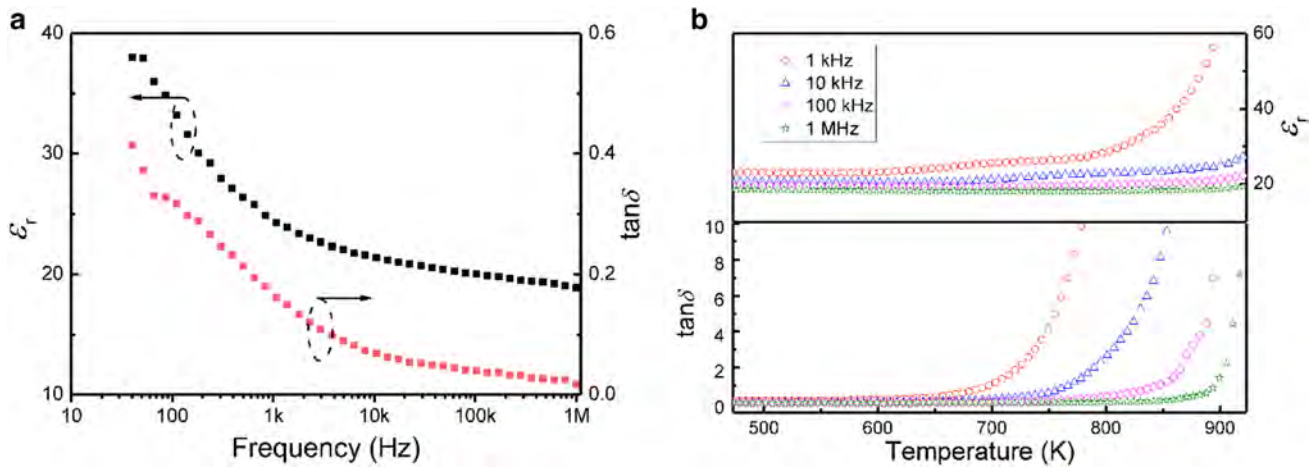

Fig. 4 Frequency and temperature dependence of dielectric permittivity and loss tangent at RF band from 100 Hz to 1 MHz

of oxygen vacancies. Their ionization produces electrons and positively charged oxygen vacancies, as follows:

$$O_O^x \rightleftharpoons V_O^x + \frac{1}{2}O_2 \tag{2}$$

$$V_O^x \rightleftharpoons V_O^{\cdot} + e' \tag{3}$$

$$V_O^{\cdot} \rightleftharpoons V_O^{\cdot\cdot} + e' \tag{4}$$

where O_O^x represents the oxygen in the crystal lattice while V_O^x is a neutral oxygen vacancy and $V_O^{\cdot}$ and $V_O^{\cdot\cdot}$, respectively, mean primarily ionized and secondary ionized oxygen vacancies. In the present system, the Na and Bi volatilization at elevated temperatures inevitably aggravates the oxygen loss to maintain electroneutrality and stoichiometry. The adjacent positive charged oxygen vacancies and negative electrons would weakly bond together to form dipoles that can be oriented by an applied electric field and dedicates to the relative permittivity.

Complex impedance analysis of $NaBi_3V_2O_{10}$ ceramic sintered at 620 °C as a function of frequency and temperature provides another evidence of defect dipoles in terms of electrical conductivity. Over a temperature range from 563 to 64 K, the total resistance, being the intercept in the real part of impedance (Z') in Fig. 5a, significantly decreased with increasing temperature, suggesting a semiconductor nature of $NaBi_3V_2O_{10}$. The increasing conductivity can be explained by the bond break of the defect dipoles when exposed to the thermal excitation, whereby free charge carriers are generated and conduct to conductivity. The thermal activation nature of the defects is validated from the frequency dependence of the imaginary part of impedance (Z''), characterized by a high-frequency shift of the peak frequency with increasing temperature. By applying the Arrhenius law to the relaxation frequency, $f = f_0 \exp(-E_a/k_B T)$ with E_a for the activation energy, k_B is the Boltzmann constant and T for the Kelvin temperature, a linear relationship between the ln f and $1/T$ was presented, as shown in Fig. 5c. Additionally, an activation energy $E_a \sim 0.95$ eV was obtained, which is close to the activation energy of the charged oxygen vacancies [41]. The optical bandgap $E_g \sim 3.05$ eV, being a direct transition between valence and conduction band, was estimated from the UV–Vis spectroscopy (Fig. 5d) based on the relation $\alpha^2 = B(h\nu - E_g)$ with a as the absorption coefficient, $h\nu$ the photon energy, and B a constant. The activation energy $E_a \sim 0.95$ eV is much lower than the half of bandgap E_g, which reveals that the observed conductivity in $NaBi_3V_2O_{10}$ originates from the extrinsic carriers, i.e., electrons and the charged oxygen vacancies in this system. In summary, it is safe to conclude that the oxygen vacancies caused by high-temperature firing and worsened by Na and Bi volatilization are responsible for the low-quality factor (or high dielectric loss). Consequently, it is believed that the dielectric properties of $NaBi_3V_2O_{10}$ would be improved through processing and compositional optimizations, which will be in-depth research in our future work.

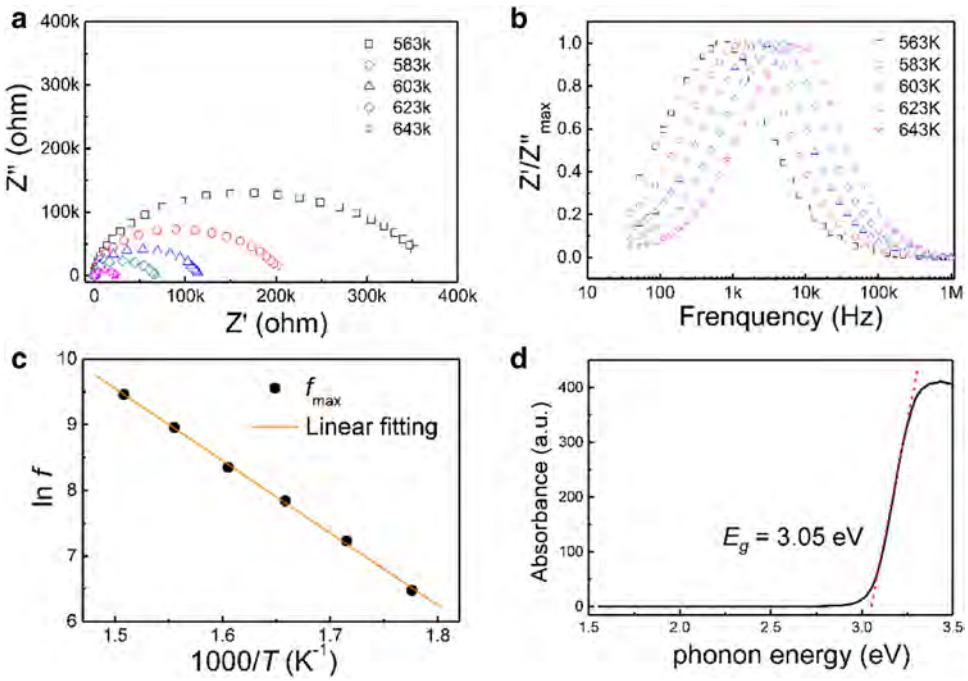

Fig. 5 **a** Complex impedance spectroscopy over a temperature range of 563–643 K; **b** the normalized imaginary part of complex impedance (Z'') at different temperatures; **c** the Arrhenius plot for the relaxation frequency; **d** UV–Vis spectroscopy of $NaBi_3V_2O_{10}$

4 Conclusions

In summary, $NaBi_3V_2O_{10}$ ceramics were prepared by the conventional solid-state reaction method at ultra-low temperatures from 600 to 640 °C. The combined microwave dielectric properties were obtained at 620 °C with $\varepsilon_r \sim 26.0$, $Q \times f \sim 3200$ GHz, and $\tau_f \sim -88.3$ ppm/°C. It should be noted that the $NaBi_3V_2O_{10}$ ceramic has good chemical compatibility with the Al electrode. The RF dielectric characterization and complex impedance analysis indicate oxygen vacancies play an adverse role in affecting the dielectric properties and Na and Bi volatilization further deteriorates the quality factor. It is expected the microwave dielectric properties can be optimized by processing and compositional optimizations.

Acknowledgements The authors acknowledge the Natural Science Foundation of Guangxi Zhuang Autonomous Region (No. 2018GXNSFAA281253), Natural Science Foundation of China (Nos. 51502047 and 51662028), and high-level innovation team and outstanding scholar program of Guangxi institutes for the financial supports.

References

1. M.T. Sebastian, *Dielectric materials for wireless communication* (Elsevier, Oxford, 2008)
2. C.C. Li, H.C. Xiang, M.Y. Xu, Y. Tang, L. Fang, Li_2AGeO_4 (A = Zn, Mg): two novel low-permittivity microwave dielectric ceramics with olivine structure. J. Eur. Ceram. Soc. **38**, 1524–1528 (2018)
3. S. George, M.T. Sebastian, Synthesis and microwave dielectric properties of novel temperature stable high Q, $Li_2ATi_3O_8$ (A = Mg, Zn) ceramics. J. Am. Ceram. Soc. **30**, 2585–2592 (2010)
4. Q.B. Lin, K.X. Song, B. Liu, H.B. Bafrooei, D. Zhou, W.T. Su, F. Shi, D.W. Wang, H.X. Lin, I.M. Reaney, Vibrational spectroscopy and microwave dielectric properties of $AY_2Si_3O_{10}$ (A = Sr, Ba) ceramics for 5G applications. Ceram. Int. **46**, 1171–1177 (2020)
5. G. Wang, Q.Y. Fu, H. Shi, F. Tian, P.J. Guo, L. Yan, S.J. Yu, Z.P. Zheng, W. Luo, Novel thermally stable, high quality factor $Ba_4(Pr_{0.4}Sm_{0.6})_{28/3}Ti_{18-y}Ga_{4y/3}O_{54}$ microwave dielectric ceramics. J. Am. Ceram. Soc. **103**, 2520–2527 (2020)
6. D. Zhou, L.X. Pang, D.W. Wang, C. Li, B.B. Jin, I.M. Reaney, High permittivity and low loss microwave dielectrics suitable for 5G resonators and low temperature co-fired ceramic architecture. J. Mater. Chem. C **5**, 10094–10098 (2017)
7. Z.Y. Zou, X.K. Lan, W.Z. Lu, G.F. Fan, Novel high Curie temperature $Ba_2ZnSi_2O_7$ ferroelectrics with low-permittivity microwave dielectric properties. Ceram. Int. **42**, 16387–16391 (2016)
8. C.Z. Yin, Y. Tang, J.Q. Chen, C.C. Li, L. Fang, F.H. Li, Y.J. Huang, Phase evolution, far-infrared spectra, and ultralow loss microwave dielectric ceramic of $Zn_2Ge_{1+x}O_{4+2x}$ ($-01 \le x \le 02$). J. Mater. Sci: Mater. Electron. **30**, 16651–16658 (2019)
9. C.Z. Yin, H.C. Xiang, C.C. Li, H. Porwal, L. Fang, Low-temperature sintering and thermal stability of Li_2GeO_3-based microwave dielectric ceramics with low permittivity. J. Am. Ceram. Soc. **101**, 4608–4614 (2018)
10. X.Q. Song, W. Lei, Y.Y. Zhou, T. Chen, S.W. Ta, Z.X. Fu, W.Z. Lu, Ultra-low fired fluoride composite microwave dielectric ceramics and their application for $BaCuSi_2O_6$-based LTCC. J. Am. Ceram. Soc. **103**, 1140–1148 (2020)
11. G. Subodh, M.T. Sebastian, Glass-free $Zn_{2T}e_3O_8$ microwave ceramic for LTCC applications. J. Am. Ceram. Soc. **90**, 2266–2268 (2010)
12. M.T. Sebastian, H. Jantunen, Low loss dielectric materials for LTCC applications: a review. Int. Mater. Rev. **53**, 57–90 (2008)
13. J.J. Bian, D.W. Kim, K.S. Hong, Glass-free LTCC microwave dielectric ceramics. Mater. Res. Bull. **40**, 2120–2129 (2005)
14. C.Z. Yin, C.C. Li, G.J. Yang, L. Fang, Y.H. Yuan, L.L. Shu, J. Khaliq, $NaCa_4V_5O_{17}$: A low-firing microwave dielectric ceramic with low permittivity and chemical compatibility with silver for LTCC applications. J. Eur. Ceram. Soc. **40**, 386–390 (2020)
15. D. Zhou, C.A. Randall, L.X. Pang, H. Wang, X.G. Wu, J. Guo, G.Q. Zhang, L. Shui, X. Yao, Microwave dielectric properties of $Li_2(M^{2+})_2Mo_3O_{12}$ and $Li_3(M^{3+})Mo_3O_{12}$ (M = Zn, Ca, Al, and In) lyonsite-related-type ceramics with ultra-low sintering temperatures. J. Am. Ceram. Soc. **94**, 802–805 (2011)
16. C.C. Chou, C.S. Chen, P.C. Wu, K.C. Feng, L.W. Chu, Influence of glass compositions on the microstructure and dielectric properties of low temperature fired $BaTi_4O_9$ microwave material with copper electrodes in reducing atmosphere. Ceram. Int. **38**, S159–S162 (2012)
17. H.C. Xiang, L. Fang, W.S. Fang, Y. Tang, C.C. Li, A novel low-firing microwave dielectric ceramic $Li_2ZnGe_3O_8$ with cubic spinel structure. J. Eur. Ceram. Soc. **37**, 625–629 (2017)
18. S.H. Yoon, D.W. Kim, S.Y. Cho, K.S. Hong, Investigation of the relations between structure and microwave dielectric properties of divalent metal tungstate compounds. J. Eur. Ceram. Soc. **26**, 2051–2054 (2006)
19. C.F. Xing, J. Bao, Y.F. Sun, J.J. Sun, H.T. Wu, Ba_2BiSbO_6: A novel microwave dielectric ceramic with monoclinic structure. J. Alloys Compd. **782**, 754–760 (2019)
20. C.C. Li, C.Z. Yin, J.Q. Chen, H.C. Xiang, Y. Tang, L. Fang, Crystal structure and dielectric properties of germanate melilites $Ba_2MGe_2O_7$ (M = Mg and Zn) with low permittivity. J. Eur. Ceram. Soc. **38**, 5246–5251 (2018)
21. C.C. Li, Z.H. Wei, H. Luo, L. Fang, Sintering behavior and microwave dielectric properties of $LiMVO_4$ (M = Mg, Zn). J. Mater. Sci: Mater. Electron. **26**, 9117–9121 (2015)
22. J.W. Chen, C.C. Li, D. Wang, H.C. Xiang, L. Fang, Preparation, crystal structure, and dielectric characterization of $Li_2W_2O_7$ ceramic at RF and microwave frequency range. J. Adv. Dielectr. **7**, 1720001 (2017)
23. H.C. Yang, S.R. Zhang, H.Y. Yang, Y. Yuan, E.Z. Li, $Gd_2Zr_3(MoO_4)_9$ microwave dielectric ceramics with trigonal structure for LTCC application. J. Am. Ceram. Soc. **103**, 1131–1139 (2019)
24. D.C. Sinclair, C.J. Watson, R.A. Howie, J.M. Skakle, A.M. Coats, C.A. Kirk, E.E. Lachowski, J. Marr, $NaBi_3V_2O_{10}$: a new oxide ion conductor. J. Mater. Chem. C **8**, 281–282 (1998)
25. R. Bliesner, S. Uma, A. Yokochi, A. Sleight, Structure of $NaBi_3V_2O_{10}$ and implications for ionic conductivity. Chem. Mater. **13**, 3825–3826 (2001)
26. D.G. Porob, T. Guru Row, A novel oxide ion conductor in a doped Bi_2O_3–V_2O_5 system: Ab initio structure of a new polymorph of $NaBi_3V_2O_{10}$ via powder X-ray diffraction. Chem. Mater. **12**, 3658–3661 (2000)
27. D. Zhou, L.X. Pang, D.W. Wang, I.M. Reaney, $BiVO_4$ based high k microwave dielectric materials: a review. J. Mater. Chem. C **6**, 9290–9313 (2018)
28. H.D. Xie, H.H. Xi, F. Li, C. Chen, Microwave dielectric properties of $BiMg_2VO_6$ ceramic with low sintering temperature. J. Inorg. Mater **30**, 202–206 (2015)
29. C. Kai, C.C. Li, H.C. Xiang, Y. Tang, Y. Sun, L. Fang, Phase formation and microwave dielectric properties of $BiMVO_5$ (M = Ca, Mg) ceramics potential for low temperature c-fired ceramics application. J. Am. Ceram. Soc. **102**, 362–371 (2019)

30. H.F. Zhou, K.G. Wang, W.D. Sun, X.L. Chen, H. Ruan, Phase composition, singtering behavior and microwave dielectric properties of $M_2BiLi_2V_3O_{12}$ (M = Zn, Ca) low temperature co-fired ceramics. Mater. Lett. **217**, 20–22 (2018)
31. J. Li, C.C. Li, Z.H. Wei, Y. Tang, C.X. Su, L. Fang, Microwave dielectric properties of a low-firing $Ba_2BiV_3O_{11}$ ceramic. J. Am. Ceram. Soc. **98**, 683–686 (2015)
32. Y. Tang, X.W. Jiang, H.C. Xiang, C.C. Li, L. Fang, X.R. Xing, Two novel low-firing $Na_2AMg_2V_3O_{12}$ (A = Nd, Sm) ceramics and their chemical compatibility with silver. Ceram. Int. **43**, 2892–2898 (2017)
33. H.C. Xiang, L. Fang, X.W. Jiang, C.C. Li, Low-firing and microwave dielectric properties of $Na_2YMg_2V_3O_{12}$ ceramic. Ceram. Int. **42**, 3701–3705 (2016)
34. X.W. Jiang, L. Fang, H.C. Xiang, H.H. Guo, J. Li, C.C. Li, A novel low-firing microwave dielectric ceramic $NaMg_4V_3O_{12}$ and its chemical compatibility with silver electrode. Ceram. Int. **41**, 13878–13882 (2015)
35. L. Fang, F. Xiang, C.X. Su, H. Zhang, A novel low firing microwave dielectric ceramic $NaCa_2Mg_2V_3O_{12}$. Ceram. Int. **39**, 9779–9783 (2013)
36. M. Rakhi, G. Subodh, Crystal structure and microwave dielectric properties of $NaPb_2B_2V_3O_{12}$ (B = Mg, Zn) ceramics. J. Eur. Ceram. Soc. **38**, 4962–4966 (2018)
37. H.F. Zhou, Y.B. Miao, J. Chen, X.L. Chen, F. He, D.D. Ma, Sintering characteristic, crystal structure and microwave dielectric properties of a novel thermally stable ultra-low-firing $Na_2BiMg_2V_3O_{12}$ ceramic. J. Mater. Sci.: Mater. Electron. **25**, 2470–2474 (2014)
38. H.C. Xiang, Y. Tang, L. Fang, H. Porwal, C.C. Li, A novel ultra-low temperature cofired $Na_2BiZn_2V_3O_{12}$ ceramic and its chemical compatibility with metal electrodes. J. Mater. Sci.: Mater. Electron. **28**, 1508–1513 (2017)
39. R.D. Shannon, Dielectric polarizabilities of ions in oxides and fluorides. J. Appl. Phys. **73**, 348–366 (1993)
40. M. Rocha, P. Silva, K. Theophilo, E. Sancho, P. Paula, M. Silva, S. Honorato, A. Sombra, High dielectric permittivity in the microwave region of $SrBi_2Nb_2O_9$ (SBN) added La_2O_3, PbO and Bi_2O_3, obtained by mechanical alloying. Phys. Scr. **86**, 025701 (2012)
41. I. Tanaka, F. Oba, K. Tatsumi, M. Kunisu, M. Nakano, H.J.M.T. Adachi, Theoretical formation energy of oxygen-vacancies in oxides. Mater. Trans. **43**, 1426–1429 (2002)